A single molecule DNA flow stretching microscope for undergraduates

Kelly Williams and Brendan Grafe
Department of Biology, Emmanuel College, Boston, Massachusetts 02115

Kathryn M. Burke
Department of Mathematics, Emmanuel College, Boston, Massachusetts 02115

Nathan Tanner and Antoine M. van Oijen
Zernike Institute for Advanced Materials, University of Groningen, Groningen, The Netherlands 9700 AB

Joseph Loparo
Department of Biological Chemistry and Molecular Pharmacology, Harvard Medical School, Boston, Massachusetts 02115

Allen C. Price[a)]
Department of Chemistry and Physics, Emmanuel College, Boston, Massachusetts 02115

(Received 15 April 2011; accepted 11 July 2011)

The design of a simple, safe, and inexpensive single molecule flow stretching instrument is presented. The instrument uses a low cost upright microscope coupled to a webcam for imaging single DNA molecules that are tethered in an easy to construct microfluidic flow cell. The system requires no special vibration isolation and is capable of measuring DNA replication at the single molecule level. We discuss two laboratory experiments suitable for advanced undergraduates using our microscope. © *2011 American Association of Physics Teachers.*
[DOI: 10.1119/1.3620410]

I. INTRODUCTION

Much of current biophysics research is concerned with the trapping and measuring of single molecules. A variety of techniques, including optical trapping, magnetic tweezers, and flow stretching have been used to study DNA replication, RNA folding, protein folding, and gene translation.[1,2] It is, therefore, desirable to increase student exposure to these important techniques. Optical trapping is one technique for which instrumentation and experiments suitable for advanced undergraduates have been developed.[3] In addition, the technique has been successfully integrated into an advanced undergraduate laboratory course.[4] Because of the elegance of the optical trapping technique, many biophysicists are well acquainted with it. However, the stringent optical requirements, which increase cost and complexity, and the use of lasers, which introduce safety issues, limit the widespread use of the technique.

The single molecule flow stretching technique has been used by biophysicists for almost a decade to study DNA replication.[5] In this technique, a fluid drag force is used to manipulate a bead attached to a surface tethered DNA in a microfluidic flow cell. Sub-piconewton forces can be applied using commercially available syringe pumps, which can reach flows as low as a few nanoliters per minute. Bead motion is measured by video microscopy and particle tracking, which can yield submicron accuracy in bead position with low magnification optics.[6]

In this paper, we describe a single molecule DNA flow stretching microscope suitable for an advanced undergraduate laboratory. By using a video camera for data acquisition and a low cost upright microscope for the optics, we achieve submicron spatial resolution of the bead position using particle tracking at video frame rates. The cost of our instrument is less than $3500, with the microscope the major cost. We begin by describing the instrument and then describe two experiments. In the first experiment, the entropic elasticity of DNA is measured. The data can be analyzed by students to either calibrate the instrument or to measure the persistence length and the bending rigidity of DNA. In the second experiment, the motion of a molecular motor, the $\phi 29$ DNA polymerase, is measured. Students measure the rate of motion of the molecular motor along the DNA as well as the total distance the motor moves along the DNA. In addition to exposing students to the physics of DNA and molecular motors, these experiments instruct students in video data acquisition, microfluidics, and molecular tethering.

II. INSTRUMENT DESIGN

In the flow stretching technique, a micro bead is attached to the free end of a surface tethered, linear DNA molecule. A flow induced drag force on the bead stretches the DNA in the flow direction. Changes in the end-to-end extension of the DNA are measured by observing changes in the position of the bead. We begin by describing the DNA tethering and bead attachment, followed by flow control, video microscopy, and other important instruments.

A. DNA tethering

Central to this technique is the tethering of the DNA to both the surface and the micro bead. As shown in Fig. 1, one end of the DNA is attached to a glass cover slip, which forms the bottom of the flow channel, and the other end is attached to a micro bead, which allows for manipulation and visualization of the DNA. The attachment points are created using molecular linkers, which bind both the functionalized surfaces and the labeled DNA. Detailed methods for preparing the functionalized glass cover slips, micro beads, and DNA are provided in Ref. 7. These materials can be prepared in advance and stored for months. Here, we shall discuss only the major points, starting with the glass cover slip, the DNA preparation, and the bead functionalization. Functionalized

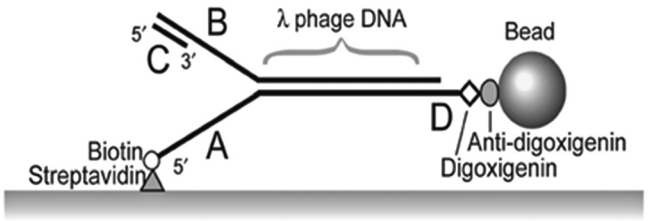

Fig. 1. Tethering of DNA and bead (not to scale). The 5′ end of the DNA (labeled A) is labeled with a biotin moiety that binds to the streptavidin, which coats the glass coverslip surface (at the bottom of the figure). The 3′ end of the DNA (labeled B) is annealed to a primer sequence (labeled C), which is necessary to initiate DNA replication. The replication fork is formed by A, B, and C. The 3′ end labeled D is covalently linked to a digoxigenin molecule that binds to the antidigoxigenin, which coats the bead. This figure is taken from Ref. 30.

glass coverslips can be purchased from some suppliers (Nanocs, Microsurfaces). We have not worked with these suppliers, and the protocols described here would likely have to be modified to work with commercially supplied materials.

To minimize non-specific interactions with the glass cover slip, we covalently couple high-molecular-weight polyethylene glycol (PEG) to the surface by first silanizing the glass surface with 3-aminopropyltriethoxysilane, which provides free amine groups that are then coupled to functionalized PEGs. By varying the ratio of biotinylated to non-biotinylated PEGs (Laysan Bio, BIO-SC-5K and M-SCM-5K), we can control the density of tethering sites for the DNA. The biotinylated PEGs tightly bind streptavidin, allowing for subsequent coupling of biotinylated DNA. Streptavidin forms tetramers with four high affinity binding sites for biotin and is often used to link biotinylated molecules.[8] We use a ratio between 50:1 and 100:1 non-biotinylated to biotinylated PEG in our reaction mixture. This ratio gives tens to hundreds of tethered DNAs in the microscope's field of view.

Bacteriophage λ DNA (New England Biolabs) contains 48,502 bases and is 16.2 μm long. It provides an ideal scaffold for single molecule DNA manipulation.[5] The linearized double stranded DNA has single-stranded overhangs, 12 bases long at each end. To these, we attach custom oligonucleotides using standard annealing and ligating techniques as described in the following.

The end of the DNA to be tethered to the cover slip, in addition to having a biotin tag, must contain a replication fork as shown in Fig. 1. A replication fork is required for the binding and activity of the DNA polymerase studied in the DNA motor protein experiment (see Sec. IV). We assemble a replication fork by annealing and ligating three custom oligonucleotides (Integrated DNA Technologies (IDT), sequences can be found in Ref. 7): (a) a biotinylated lagging strand, which links the DNA to the streptavidin on the surface, (b) a leading strand, which can function as a template in DNA replication experiments, and (c) a short primer complimentary to the 3′ end of the leading strand (see Fig. 1). Although the replication fork is not necessary for the DNA force-extension experiment (see Sec. III), it does not interfere with that experiment, and the same construct can function for both the DNA replication and the DNA force-extension experiments.

At the other end of the DNA, we anneal and ligate a digoxigenin labeled oligonucleotide (IDT, see Ref. 7 for the sequence). The digoxigenin binds to the antidigoxigenin on the bead. The digoxigenin–antidigoxigenin link is also used frequently in single molecule tethering.[5]

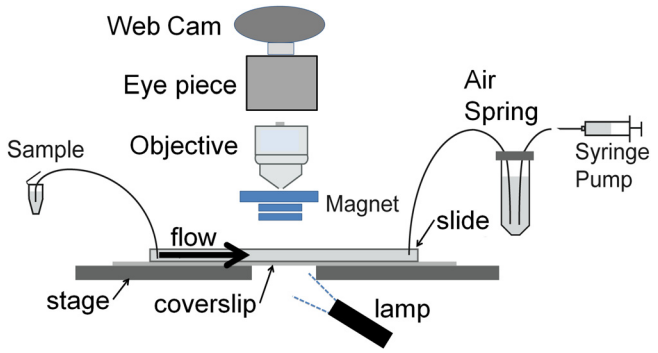

Fig. 2. Experimental setup. Buffer is drawn from the sample through the flow cell and air spring into the syringe pump. The air spring isolates the flow cell from any mechanical noise generated by uneven pump action. The tethered DNAs are in the flow cell below the magnet. The off-axis lamp below the microscope stage creates dark field imaging. The image formed by the objective and eyepiece is viewed with the webcam. For simplicity, the microscope body is not shown.

We use functionalized paramagnetic micro beads (Invitrogen, Dynabeads M-280 Tosylactivated). Following the tosyl amine coupling protocol supplied with the beads, we covalently linked the beads to antidigoxigenin Fab fragments (Roche, see Ref. 7). The fully tethered DNA, as shown in Fig. 1, is situated at the bottom of the flow channel, as described in Sec. II B.

B. Flow path

Control of the fluid drag force on the micro bead is critical, and the flow cell and the fluid path must be designed carefully. The flow path can be seen in Fig. 2. The flow is drawn with a syringe pump (Kent Scientific GENIE plus) from the sample tube through the flow cell and through an "air spring," which dampens the effects of the mechanical noise of the pump.[5,9]

As shown in Fig. 3, the flow cell is created by cutting a channel in double-sided tape and sandwiching the tape

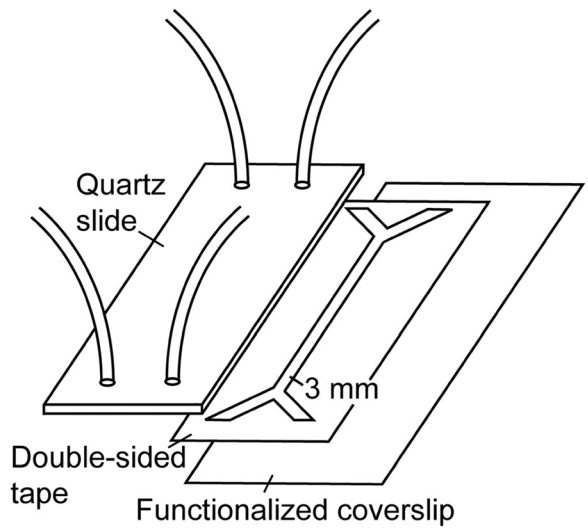

Fig. 3. Exploded view of flow cell. The flow channel is cut from double-sided tape (120 μm thick) and sandwiched between the quartz slide and the functionalized coverslip. Predrilled holes in the quartz slide match the tube diameter. The *Y*-shaped channel allows two inlet/outlet ports, which can be switched after loading beads. This figure is taken from Ref. 7.

between the functionalized cover slip and a 1 mm thick quartz or glass slide (Technical Glass Products, Painesville, OH). We use tape of thickness 120 μm (Grace Biolabs SA-S-1L) and a channel width of 3 mm for the ϕ29 DNA polymerase experiments. The outlet and inlet holes in the quartz slide must be predrilled to match the tube size. We use tubing with an outside diameter of 1.22 mm, an inside diameter of 0.76 mm (Intramedic PE60), and a 1.2 mm flame Dremel tool (DiamondBurs HP863-012) for a snug fit. Cutting the end of the tubes at a 30° angle prevents the face of the tube from sealing against the cover slip surface and blocking the flow. After inserting the tubing, we use quick setting epoxy to seal the flow cell around the edges and to secure the tubes in the holes. We use diagonally opposite ports when flowing sample through the cell as this gives a more uniform flow profile. After loading beads (described in Sec. III B), we switch inlet ports to reduce the amount of washing needed to remove free beads from the tubing. During an experiment, the outlet tube not in use is always closed, either with a shut off valve or by kinking it and securing it with tape.

The air spring is made with a 50 ml centrifuge tube filled with water to the 45 ml mark. Three holes are pierced in the lid, and three lengths of tubing are inserted to about 1 cm from the bottom. The lid and holes are sealed with epoxy. One tube connects to the syringe pump and the other two connect to the outlet lines from the flow cell.

C. Microscope and camera

We chose an upright trinocular microscope (Olympus CH30) for its low cost and ease of use. A long working distance objective (Zeiss Epiplan LWD 10×, working distance 18 mm) gives us ample room above the sample for tubing and the magnet manipulator described below. The low numerical aperture (0.24) does not significantly affect measurements because the position of the image of the 2.8 μm beads is determined by Gaussian fitting, which can yield better than diffraction limited resolution.[10]

Our video data are acquired using a webcam (Logitech Notebook Pro). A manual focus webcam allows for fixing the focus at the standard microscope image distance (approximately 250 mm). The webcam is attached to a 20× eyepiece using plastic washers as spacers to place the iris of the camera lens at the exit pupal of the eyepiece. The correct spacing to avoid vignetting was found by trial and error. The optics yields a resolution on the webcam CCD of 3.0 μm/pixel as determined using a slide micrometer. Video data are recorded using video capture software (OPEN VIDEO CAPTURE). For data collection, off-axis illumination is used to achieve dark field imaging, which creates bright spots on a dark background at the bead locations, which is necessary for the particle tracking software (see Sec. III B). We remove the condenser and place a flexible LED light (IKEA JANSJO) below the stage off axis. Larger incident angles improve the signal to background. Our geometry limited us to incident angles from 70 to 80°.

D. Magnet

To reduce non-specific interactions between the bead and the surface of the flow cell, we lift the paramagnetic beads upward using permanent magnets. A stack of three neodymium ring magnets (National Imports, NSN0814 and NSN0615) can be centered on the optical axis above the sample without blocking the image (see the geometry in Fig. 2). As determined in Sec. III, the magnets exert a force of approximately 1 pN on the bead when positioned 8 mm above the flow cell (distance measured from bottom of lowest magnet to the top surface of flow cell). The magnet force depends on the specific magnets used as well as the magnet height. A low cost vertical manipulator for the magnets can be constructed by using epoxy to fix the magnets to a ruler, which is attached to the movable jaw of a vernier caliper. The caliper is held by a ring stand, which is moved manually to center the magnets above the sample.

III. EXPERIMENT: DNA FLOW STRETCHING

The experiment described in this section serves two purposes. It can be used to calibrate the force that the magnets exert on the paramagnetic bead. Knowledge of the magnitude of this force is necessary prior to performing any molecular motor experiments. It also can be used to measure the bending rigidity of DNA. We will frame our discussion in terms of the calibration and then explain how the other purpose can be served with the same procedure. We first present the theoretical analysis of the experiment, followed by a description of the experiment and the interpretation of the data.

A. Theory

The analysis of this experiment provides a beautiful application of mechanical equilibrium. It also serves as an excellent introduction to the analysis of micro-flows, as well as to the worm-like chain model of polymer physics.

A model of the tethered DNA is shown in Fig. 4. For a given magnetic force and fluid drag force on the bead, the condition for static equilibrium is

$$\vec{f}_m + \vec{f}_d - t\hat{r} = 0, \tag{1}$$

where $\vec{f}_m$ is the force due to the magnet, $\vec{f}_d$ is the drag force due to the fluid flow, t is the tension in the DNA, and $\hat{r}$ is the unit vector pointing from the tethering point on the surface toward the bead.

We assume the magnetic force is constant and independent of position, and the drag force can be calculated using the Stokes relation,[11]

$$\vec{f}_d = 6\pi\eta R\vec{v}(\vec{r}), \tag{2}$$

where R is the radius of the spherical bead, η is the dynamic viscosity of the fluid, and $\vec{v}(\vec{r})$ is the velocity field describing

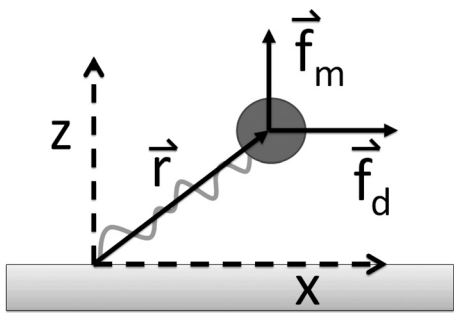

Fig. 4. Model of the tethered DNA and bead. The flow direction is to the right. The position of the bead center is $\vec{r}$. The magnet force and the fluid drag force are $\vec{f}_m$ and $\vec{f}_d$, respectively. The functionalized coverslip is in the x - y plane.

the flow. For non-uniform flow fields, such as those very close to the glass cover slip surface, Eq. (2) must be corrected by Faxen's law.[12] This correction can be shown to be small in our case.

The flow field in the channel (see Appendix A) is given by

$$v_x(z) = 4v_{\max}\frac{z}{h}\left(1-\frac{z}{h}\right), \tag{3}$$

where

$$v_{\max} = \frac{3Q}{2wh}. \tag{4}$$

In these equations, the x direction is defined as parallel to the long dimension of the channel in the flow direction, v_x is the x component of the fluid velocity, z is the height above the glass cover slip, h is the thickness of the channel (120 μm in our case), w is the width of the channel (6 mm in the calibration experiment, see below), and Q is the volume flow rate as set on the syringe pump controls. The y and z components of the fluid velocity are zero.

The tension in the DNA can be determined from the force-extension relation for double stranded DNA (labeled dsDNA in Fig. 5). This relation can be numerically calculated from the worm-like chain model.[13] The following interpolation formula[13] is adequate for our purposes:

$$t = \frac{k_B T}{\ell_P}\left\{\frac{1}{4\left(1-\frac{d}{L}\right)^2}-\frac{1}{4}+\frac{d}{L}\right\}, \tag{5}$$

where k_B is Boltzmann's constant, T is the temperature, ℓ_P is the persistence length of the DNA, L is the contour length, and d is the end-to-end extension of the DNA. The persistence length quantifies the rigidity of the DNA and is related to the bending rigidity, κ, by

$$\ell_P = \frac{\kappa}{k_B T}. \tag{6}$$

The persistence length of DNA has been measured to be 53 nm,[14] corresponding to a bending rigidity of 219 pN nm^2. Equation (5) is valid for $L \gg \ell_P$ and $t < 5$ pN, conditions which hold in the experiments we describe. To take into consideration the finite size of the bead we must use $d = r - R$, where R is the bead radius, and r is the measured distance of the bead from the surface attachment point of the DNA.

In principle, by solving Eqs. (1)–(5), we can determine the bead position for any volume flow rate and magnet force. The non-linearity of Eq. (5) makes an analytical solution difficult. This problem provides an excellent opportunity to illustrate the use of numerical techniques. Our solution to the problem is a short program (described in Appendix B) that calculates the bead position given the magnet and fluid drag forces. Figure 6 shows the output of this program for various flow rates and magnet forces. Input flow rate is plotted on the vertical axis, and the horizontal component of the bead position on the horizontal axis for different values of the magnetic force. This method of plotting the calculations makes comparison with the experimental measurements straightforward; because it is the horizontal displacement of the bead which is measured (the vertical component is parallel to the optic axis). Note that the magnetic force strongly effects the slope at low flow rates. The large flow rate limit is determined by the contour length of the DNA (16.2 μm in our case).

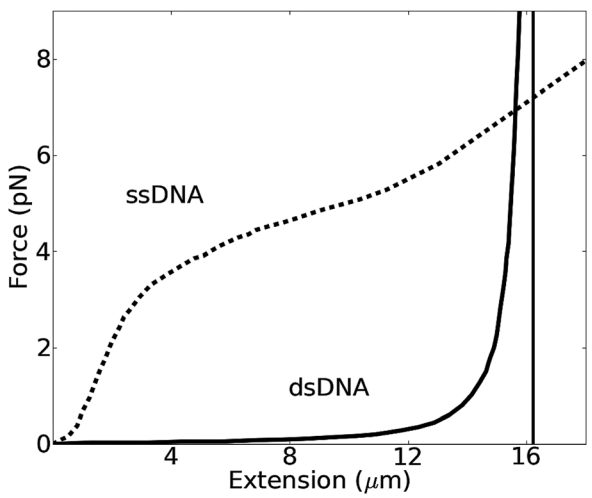

Fig. 5. DNA force-extension relation. The difference in extension for double stranded DNA (dsDNA) and single stranded DNA (ssDNA) is evident in this plot. This figure is adapted from Ref. 7.

B. Materials and methods

For a successful magnetic force calibration, we need to apply forces less than 1 pN. To reduce the drag force for a given flow rate, we use a wide channel flow cell (width 6 mm). The air spring is not critical for these measurements, and we performed this experiment without it.

After assembly of the flow cell and insertion into the flow path (described previously), DNA and beads must be introduced. To bind the DNA, we dilute between 0.5 and 2 μl of DNA stock (prepared following the protocol in Sec. II A) into between 1 and 1.5 ml of working buffer (20 mM Tris pH

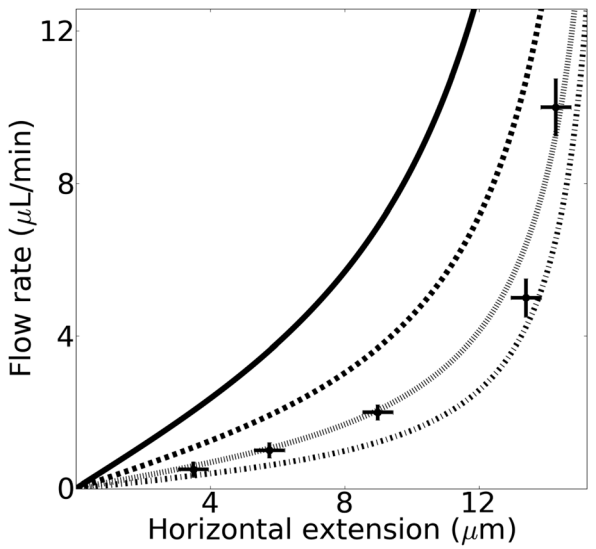

Fig. 6. DNA flow extension: comparison of experiment and theory. The horizontal bead position is plotted on the horizontal axis and the flow rate on the vertical. The curves show the calculation for four magnetic forces: 4 pN (solid line), 2 pN (dashed line), 1 pN (dotted line), and 0.5 pN (dash-dotted line). The measured values are shown with uncertainties. Uncertainties in the flow rate are assumed to be 10% (from the pump manufacturer's specifications), and those of the horizontal extension are from standard deviations of the measured bead trajectories.

7.5, 2 mM EDTA, 50 mM NaCl). This solution is pumped through the flowcell at a flow rate from 20 to 40 μl/min. The concentration and flow rate can be adjusted to optimize the binding efficiency. The numbers we have given should give a few tens to hundreds of tethered beads in the field of view. After the DNA, the beads are flowed at a rate of 10 to 20 μl/min. We use 2 to 3 μl of bead stock (prepared following the protocol in Sec. II A) diluted in 1 ml of blocking buffer (20 mM Tris pH 7.5, 2 mM EDTA, 50 mM NaCl, 1 mg/ml bovine serum albumin (BSA), and 0.025% Tween-20 (a detergent)). The bead solution must be thoroughly mixed on a vortexer and sonicated before use to break up aggregates. After loading the beads, there should be many tethered DNA-bead assemblies in the field of view. Tethered beads and DNA can be identified by gently tapping the outlet tube while the flow is on. Properly tethered beads will move in response to the flow disruption and then return to their previous positions. Normally, a number of beads will stick to the bottom of the flow cell non-specifically. These can be removed by washing the flow cell (10 to 20 μl/min for 30 min) with blocking buffer while tapping the microscope stage. Before washing with buffer, the inlet/outlet tubes should be switched, because beads stick to the inside of the tubing. After bead binding, the DNA-bead assemblies are extremely sensitive to flow in the chamber. From this point on, whenever samples or tubes are switched, all outlet tubes must be sealed off to prevent hydrostatically driven flow through the chamber. Once the flow cell has been washed, the magnet to be calibrated can be introduced.

The magnet can be tested by bringing it in from the side toward the flow cell while simultaneously viewing the beads either through the eyepiece or from the webcam. The beads will move toward a suitable magnet without breaking off from the surface. Breaking indicates too large a magnet force. If the beads do not move in response to the magnet, the force is too weak. Once a suitable magnet has been chosen, it can be mounted in a vertical manipulator (see Sec. II D for a description of a low cost option) and centered above the sample.

A minimum of five flow rates should be measured. For each data point, we collect video data for 4 to 5 min per flow rate, at 2 frames per second. The flow rate is first set to zero and then data collection is started. The flow is then turned on for about 1 min after the video collection starts and is turned off at about 1 min before data collection stops. This procedure is used to identify the baseline and to spot drift. We find that drift is negligible, because the beads always returned to the same position within the experimental uncertainties. The initial data processing step in this experiment introduces students to particle tracking, an important method in biophysics. We process data with the MOSAIC particle tracker plugin for ImageJ.[15] The horizontal component of the end-to-end extension of the DNA is determined by averaging the bead position during flow and subtracting the average position during zero flow. The measurement in pixels is then converted to microns using the previously determined spatial resolution of the camera (see Sec. II C).

C. Results

A plot of the horizontal extension of the DNA versus the flow rate for a bead is shown in Fig. 6. The solid curves in Fig. 6 show the theoretical horizontal extension of the DNA as calculated using the program described in Appendix B. Fitting the program output to the data was achieved by calculating the curve for various values of the magnetic force and overlaying the calculated curve on the data. The closest fit was chosen by eye. The uncertainty in the value of the magnetic force can be determined by varying the magnetic force in the script, recalculating the curve and comparing with the data to find the values that are not consistent with the data. In this way, the magnetic force was found to be 1.0 ± 0.2 pN.

The value of the magnetic force obtained in this way depends on the value assumed for the persistence length of the DNA. In our calculation, we assumed $\ell_P = 53$ nm.[14] This experiment cannot be used to determine both the magnetic force and the persistence length simultaneously. If desired, we can calibrate the magnet as described, and then give that force value to students at the start of the laboratory. Student would then perform the same experimental procedure outlined previously and then vary the persistence length in the analysis until the calculated curve matches the data. In this way, students determine the persistence length of DNA. Of course, the two experiments taken together are circular and do not constitute a genuine measurement of the persistence length. However, this fact would not be obvious to students, because they would not participate in the calibration. An actual determination of the persistence length of DNA requires an independent calibration of the magnet force as is discussed in Sec. V.

IV. EXPERIMENT: DNA REPLICATION

In this section, we describe the measurement of the motion of a molecular motor protein along a single DNA strand. We start with a general discussion of molecular motors and explain the principles behind our experimental technique. We then describe the experimental protocol and data analysis and present some example data and their interpretation.

A. Theory

Research into molecular motors is an active area of biophysics to which undergraduates have little exposure in laboratory courses. Molecular motors are enzymatic molecules that convert chemical energy into motion.[16] Processive motor proteins step unidirectionally along linear tracks while hydrolyzing nucleoside triphosphates.[17] These motors are characterized by their rate of motion along the DNA and by how far along the DNA the motor moves before dissociating. This latter quantity is termed the *processivity* of the motor. An important class of motor proteins move along DNA and perform enzymatic activities such as DNA unwinding (helicases), base pair removal (exonucleases), and DNA replication (DNA replicases).[18] Many of the DNA motor proteins, including the three types we have mentioned, have the effect of converting double stranded DNA (dsDNA) to single stranded DNA (ssDNA). For example, in DNA replication if only one strand is replicated, then the strand complementary to the template DNA is left in a single stranded state as the motor protein moves along the DNA.

We can take advantage of the distinct mechanical behaviors of dsDNA and ssDNA to measure the progress of such DNA motor proteins using the flow stretching technique.[19] Figure 5 shows that if the tension in the DNA is held between 2 and 3 pN, then the end-to-end extension of the DNA will dramatically decrease as the dsDNA converts to

ssDNA. This decrease in the end-to-end extension results in observable motion of the tethered bead.

Important to this technique is controlling the DNA tension. The tension in the DNA can be calculated, assuming the flow rate and magnetic force are known, using a program such as that described in Appendix B. The calculation of the flow rate necessary to yield a tension between 2 and 3 pN forms the basis for an excellent pre-lab assignment. We assume a magnetic force of 1.0 pN (see Sec. III C) and chose a flow rate of 12.5 μl/min. This force gives a tension in the DNA of 2.5 pN, as calculated by our program.

To properly interpret the data, the change in bead position must be converted to the number of base pairs (bp) of DNA processed. We can use the data shown in Fig. 5 to do this conversion. At 2.5 pN, the data show the extension of the dsDNA to be 15.0 μm, and that of the ssDNA to be 2.3 μm. Therefore, to convert the distance of the bead movement to the base pairs processed, we divide the total length of the DNA in base pairs by the change in extension, that is,

$$\frac{48502\text{bp}}{(15.0-2.3)\mu\text{m}} \approx 3820\frac{\text{bp}}{\mu\text{m}}. \tag{7}$$

The rates of movement along the DNA can then be determined by fitting the slopes of the bead trajectories. Additionally, processivities can be determined by measuring the total distance the bead moves during a single event.

This analysis is applicable to any DNA molecular motor which converts dsDNA to ssDNA. In the following, we describe the application of the technique to the measurement of DNA replication.

B. Materials and methods

The DNA polymerase (DNAP) used in this experiment is the replicative polymerase from the ϕ29 bacteriophage genome. It is commercially available, highly processive, and widely used in biotech applications.[20] The mechanism of DNA replication is an excellent example of how molecular machines work, and its study gives students an opportunity to learn about this fascinating topic in molecular biology.[21]

The preparation of the flow cell and DNA tethering is as described in Sec. III B. In this experiment, we use a channel 3 mm in width and insert the air spring in the flow path as shown in Fig. 2.

Once the DNA and beads are tethered, the ϕ29 DNAP sample must be prepared. We purchased our ϕ29 DNA polymerase (New England Biolabs) and followed the supplier's protocol. We dilute 0.5 μl of the enzyme as supplied into 450 μl of reaction buffer (50 mM Tris-HCl, 10 mM $(NH_4)2SO_4$, 10 mM MgCl2 4 mM Dithiothreitol pH 7.5, supplied), and add dNTPs to 200 μM, and BSA to 200 μg/ml, resulting in a total sample volume of 500 μl. The reaction mixture is flowed through the cell at 12.5 μl/min for approximately 30 min.

DNA replication begins as soon as the reaction mixture reaches the flow cell. Video data, at a frame rate of 2 Hz, should be started immediately and collected over the entire 30 min. The resulting video file is processed using ImageJ as described in Sec. III B. Analysis of the particle trajectories was performed by importing the data into LOGGERPRO[22] and using the software's linear fitting and statistical analysis tools.

C. Results

Typically, many trajectories from an experiment will be of stuck beads that show flat trajectories, as well as outliers that are difficult to interpret due to beads sticking during the experiment or beads breaking off. Good trajectories are easy to spot by their shape (see Fig. 7). A good way to confirm good trajectories is to reverse the flow direction briefly at the beginning of data collection, as can be done simply by lifting the air spring. Good trajectories will clearly show this flow reversal event.

A linear fit to the sloped central region for the data shown in Fig. 7 gives the slope as 0.0028 pixels/frame. If we use the known resolution of the camera (3.0 μm/pixel), the distance to base pair conversion derived in Sec. IV A, and the video frame rate (2 Hz), we can determine the rate of motion of the molecular motor for this event to be 64.2 bp/s. The processivity is determined from the total change in bead position during the event. For the data shown, the change is 2.4 pixels, which converts to 27,500 bp.

Figure 8 shows histograms of the rates and processivities from the combined results of three experiments. The rates show a roughly Gaussian distribution with a mean of 59 bp/s and a standard deviation of 19 bp/s. Examination of the raw data (see Fig. 7) shows that the uncertainty in a single rate determination is much less than this width. The width of the distribution, therefore, represents the intrinsic variation among the molecular events.

The wide distribution, typical in single molecule experiments,[23] demonstrates the power of single molecule techniques to measure the underlying distributions and not just the ensemble averages. The variation in observed rates could be due to individual molecules being in different conformations, whose lifetimes are longer than the time each molecule spends on the DNA.[24]

The histogram of processivities [see Fig. 8(b)] shows a different type of distribution. If we assume that the probability that the enzyme will dissociate from the DNA at any given step is a constant and independent of history, the probability that a given motor will reach the n th base pair is

$$P_n = p(1-p)^n, \tag{8}$$

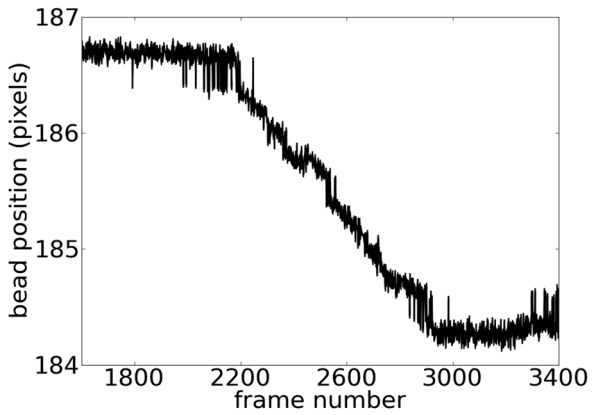

Fig. 7. Trajectory of a bead during a DNA replication experiment. The coordinate of the bead in pixels along the flow direction versus the frame number. The direction of the flow is toward increasing pixel number. The slope of the diagonal region can be converted to the rate of motion along the DNA using the conversion factors discussed in the text. The difference in height between the plateaus before and after this region can be converted to the single molecule processivity.

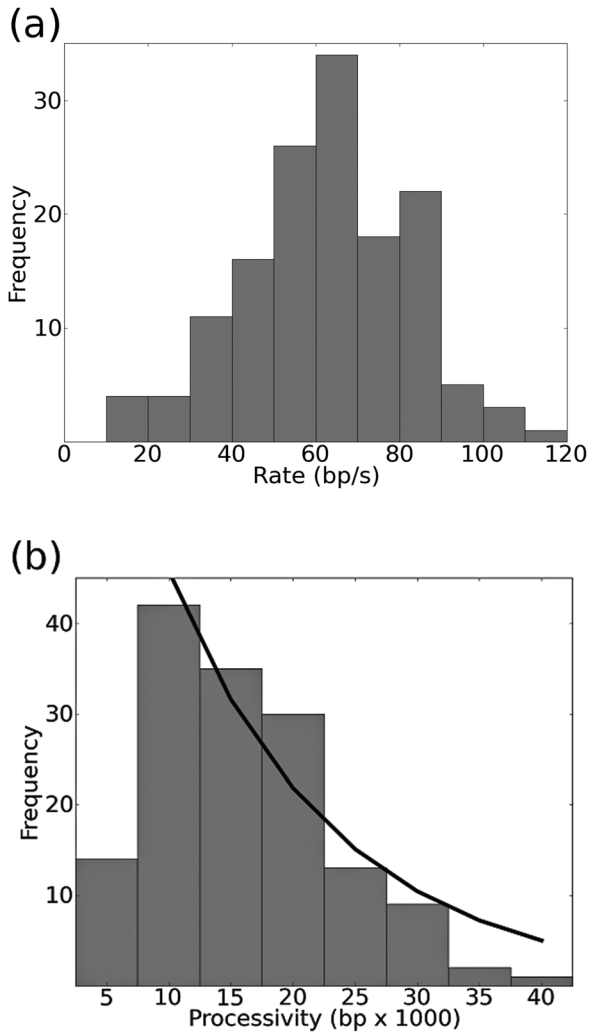

Fig. 8. Histograms of $\phi 29$ DNAP molecular motor results. Shown are the combined results of three experiments. (a) Single molecule rates. The mean speed is 59 bp/s with a standard deviation of 19 bp/s. This distribution width is a result of dispersion in the single molecule events and is not due to uncertainty in the rate determination. (b) Single molecule processivities. The data for processivities greater than 5000 bps fit to a single exponential with a decay length of 13500 bp.

where p is the probability that the motor dissociates during any given step of length one base pair. The fact that Eq. (8) predicts an exponential decay can be made explicit by defining the decay constant $k = |ln(1-p)|$. The probability can then be written as $P_n = pe^{-kn}$. By performing a simple integration, the expectation value of n can be shown to be k^{-1}. The histogram shows less than the expected number of events in the first bin (0 to 5000 bp). From Fig. 7, it can be seen that it is difficult to correctly identify events shorter than the noise level (around 0.25 pixels). This noise level corresponds to a DNA length of around 2900 bp and so could be expected to artificially reduce the number of short events. A fit of the data excluding the first bin is shown in Fig. 8b. From the fit, the probability, p, is determined to be approximately 7×10^{-5}. The mean or expectation processivity is equal to the inverse of p and is 13,500 bp.

Our results are similar to other determinations of the single molecule rates and processivities for $\phi 29$ DNAP,[25] which find similar distributions with a mean rate of 58 bp/s and a mean processivity of 17,500 bp.

V. OTHER EXPERIMENTS

The experiments we have described can be straightforwardly modified and/or extended. One modification of the force-extension experiment in Sec. III is to determine the extension curve for different lengths of DNA. The slope of the force versus extension relations at small extension is the "spring constant" of DNA and is predicted by Eq. (5) to be inversely proportional to the contour length of the DNA. Single stranded DNA (ssDNA) constructs can also be prepared and tethered and the force-extension behavior of ssDNA, which is quite different from dsDNA (see Fig. 5), can be measured.

By implementing vibration isolation, tethered Brownian motion can also be studied.[26] Our attempt to measure this effect was hindered by vibration noise, but our instrument has the time and spatial resolution required. The power spectral density of the fluctuations in the position of the bead about the equilibrium position can be fit to a Lorentzian. The fitting parameters can be related to the spring constant of the trapping force on the bead.[27] In the absence of flow, this trapping force is the vector sum of the vertical magnet force and the tension force applied to the bead by the DNA. This measurement can be used to measure the magnet force independently of the properties of the DNA and can serve as an independent calibration of the magnet force (see Sec. III).

The molecular motor experiment can be applied to other enzymes. The only requirement is that the enzyme convert dsDNA to ssDNA or *vice versa*. Two examples of processive DNA motor proteins that have been successfully studied with the flow stretching technique are helicases,[28] which unwind dsDNA and exonucleases,[5] which remove bases from one strand of a duplex DNA. Both are available commercially (New England Biolabs), and both can be studied without significant changes to the protocol.

ACKNOWLEDGMENTS

This work was made possible by the support of Emmanuel College. K.W, B.G, and K.M.B. would like to acknowledge the support of the Emmanuel College Summer Research Program. J.J.L. was supported by the Jane Coffin Childs Medical Memorial Fund and by Harvard Medical School. A.M.vO. would like to acknowledge financial support from the National Institutes of Health and the National Science Foundation.

APPENDIX A: FLUID FLOW IN MICRO-CHANNEL

The goal of this appendix is to derive Eqs. (3) and (4). The derivation is an excellent introduction to viscous flows in confined geometries, an important topic in microfluidics. The geometry is shown in Fig. 9. The flow velocity obeys the Navier–Stokes equation,

$$\frac{d\vec{v}}{dt} = \frac{\partial \vec{v}}{\partial t} + (\vec{v}\cdot\vec{\nabla})\vec{v} = \frac{\eta}{\rho}\vec{\nabla}^2\vec{v} - \frac{1}{\rho}\vec{\nabla}p, \tag{A1}$$

where $\vec{v}$ is the flow velocity, η is the dynamic viscosity, ρ is the fluid density, and p is the pressure. We assume that the flow is in the direction of the long axis of the channel; the pressure gradient is constant and in the direction of the flow, and the flow is time independent. These assumptions are expressed by

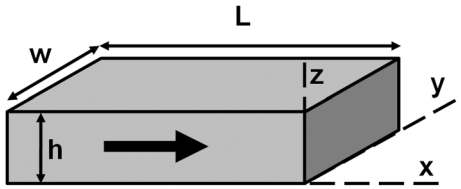

Fig. 9. The geometry of the microfluidic flow channel. Flow direction is indicated by a thick arrow. The channel height is h, the width is w, and the total length is L. Axes are oriented so that the flow is in the x direction and independent of the x coordinate.

$$\vec{v}(\vec{r}) = v_x(y,z)\hat{x}, \tag{A2}$$

$$\vec{\nabla}p = -\frac{\Delta p}{L}\hat{x}, \tag{A3}$$

$$\frac{d\vec{v}}{dt} = 0, \tag{A4}$$

where Δp is the pressure drop across the channel. These assumptions reduce the Navier–Stokes equation to

$$\frac{\partial^2 v_x}{\partial y^2} + \frac{\partial^2 v_x}{\partial z^2} = -\frac{\Delta p}{\eta L}. \tag{A5}$$

Additionally, the flow must satisfy the no slip boundary condition on the inner channel surfaces: $v_x(y,z=0) = v_x(y,z=h) = v_x(y=-w/2,z) = v_x(y=w/2,z) = 0$. The solution to this two-dimensional partial differential equation gives the flow profile in the y - z plane. For $w \gg h$, the solution to Eq. (13) is independent of y, and is given by

$$v_x(z) = 4v_{\max}\frac{z}{h}\left(1-\frac{z}{h}\right), \tag{A6}$$

where

$$v_{\max} = \frac{h^2\Delta p}{8\eta L}. \tag{A7}$$

The volume flow rate can be calculated from this model by evaluating the integral over a surface spanning the channel,

$$Q = \int \vec{v}\cdot\overrightarrow{da} = \frac{wh^3\Delta p}{12\eta L}. \tag{A8}$$

Combining Eqs. (A7) and (A8) yields the maximum fluid velocity in terms of the volume flow rate, Q,

$$v_{\max} = \frac{3Q}{2wh}. \tag{A9}$$

APPENDIX B: PROGRAM FOR CALCULATING THE BEAD POSITION

The equilibrium position of the bead is determined by numerically solving the dynamical equation,

$$\mu\frac{d\vec{r}}{dt} = \vec{f}_m + \vec{f}_d - t\hat{r}, \tag{B1}$$

where μ is the mobility of the bead, $\vec{f}_m$ is the magnetic force, $\vec{f}_d$ is the fluid drag force, t is the tension in the DNA, and $\hat{r}$ is the unit vector pointing from the tethering point on the surface toward the bead. Because the equilibrium point is stable, any trajectory starting from reasonable initial coordinates will approach the equilibrium point as $t \to \infty$.

The integration is performed by an explicit, forward step Euler method.[29] The mobility is absorbed into a scale factor (the time step in the integration), which is set small enough to produce convergence. The script takes as arguments the magnetic force and the drag force on the bead. The initial coordinates are chosen arbitrarily to be $(0.1L, 0.1L)$, where L is the contour length (16.2 μm) for λ phage DNA. Integration proceeds until convergence is reached.

We implemented this algorithm in PYTHON, a freely available and open source interpreted language.[31] PYTHON has a simple, easy to learn syntax, and there are good numerical and scientific packages available.[32]

[a]Electronic address: priceal@emmanuel.edu

[1]For an excellent review of the field, see the single molecule theme issue of Annual Reviews of Biochemistry 77 (2008).
[2]W. J. Greenleaf, M. T. Woodside, and S. M. Block, "High-resolution single-molecule measurements of biomolecular motion," Annu. Rev. Biophys. Biomol. Struct. **36**, 171–190 (2007).
[3]D. C. Appleyard, K. Y. Vandermeulen, H. Lee, and M. J. Lang, "Optical trapping for undergraduates," Am. J. Phys. **75**, 5–14 (2007).
[4]Instrumentation details as well as student protocols can be found at ⟨labs.physics.berkeley.edu/mediawiki/index.php/Optical_Trapping⟩.
[5]A. M. van Oijen, P. C. Blainey, D. J. Crampton, C. C. Richardson, T. Ellenberger, and X. S. Xie, "Single-molecule kinetics of exonuclease reveal base dependence and dynamic disorder," Science **301**, 1235–1238 (2003).
[6]M. K. Cheezum, W. F. Walker, and W. H. Guilford, "Quantitative comparison of algorithms for tracking single fluorescent particles," Biophys J. **81**, 2378–2388 (2001).
[7]N. A. Tanner and A. M. van Oijen, "Visualizing DNA replication at the single-molecule level," Methods Enzymol. **75**, 259–278 (2010).
[8]M. Wilchek, E. A. Bayer, and O. Livnah, "Essentials of biorecognition: The (strept)avidin-biotin system as a model for protein-protein and protein-ligand interaction," Immunol Lett. **103**, 27–32 (2006).
[9]P. C. Blainey, A. M. van Oijen, A. Banerjee, G. L. Verdine, and X. S. Xie, "A base-excision DNA-repair protein finds intrahelical lesion bases by fast sliding in contact with DNA," PNAS **103**, 5752–5757 (2006).
[10]A. M. van Oijen, J. Köhler, J. Schmidt, M. Müller, and G. J. Brakenhoff, "3-dimensional super-resolution by spectrally selective imaging," Chem. Phys. Lett. **292**, 183–187 (1998).
[11]R. A. Granger, *Fluid Mechanics* (Dover Publication, Mineola, NY, 1995), p.78.
[12]M. P. Sheetz, "Laser tweezers in cell biology," Methods Cell Biol. **55**, 111–112 (1998).
[13]J. F. Marko and E. D. Siggia, "Stretching DNA," Macromolecules **28**, 8759–8770 (1995).
[14]C. Bustamante, J. F. Marko, E. D. Siggia, and S. Smith, "Entropic elasticity of lambda phage DNA," Science **9**, 1599–1600 (1994).
[15]I. F. Sbalzarini and P. Koumoutsakos, "Feature point tracking and trajectory analysis for video imaging in cell biology," J. Struct. Biol. **151**, 182–195 (2005).
[16]C. Mavroidis, A. Dubey, and M. L. Yarmush, "Molecular machines," Annu. Rev. Biomed. Eng. **6**, 363–395 (2004).
[17]M. Schliwa and G. Woehike, "Molecular motors," Nature (London) **422**, 759–765 (2003).
[18]R. Seidel and C. Dekker, "Single-molecule studies of nucleic acid motors," Curr. Opin. Struct. Biol. **17**, 80–87 (2007).
[19]G. J. L. Wuite, S. B. Smith, M. Young, D. Keller, and C. Bustamante, "Single-molecule studies of the effect of template tension on T7 DNA polymerase activity," Nature (London) **404**, 103–106 (2000).
[20]R. Johne, H. Müller, A. Rector, M. van Ranst, and H. Stevens, "Rolling-circle amplification of viral DNA genomes using phi29 polymerase," Trends Microbiol. **17**, 205–211 (2009).
[21]B. Alberts, D. Bray, A. Johnson, J. Lewis, M. Raff, K. Roberts, and P. Walter, *Essential Cell Biology: An Introduction to the Molecular Biology of the Cell* (Garland Publishing, New York, 1998), pp. 189–198.
[22]Further information on LoggerPro can be obtained at ⟨www.vernier.com/soft/lp.html⟩.

[23]C. Bustamante, "In singulo biochemistry: When less is more," Annu. Rev. Biochem. **77**, 45–50 (2008).
[24]S. Kamtekar, A. J. Berman, J. Wang, J. M. Lazaro, M. de Vega, L. Blanco, M. Salas, and T. A. Steitz, "Insights into strand displacement and processivity from the crystal structure of the protein-primed DNA polymerase of bacteriophage phi29," Mol. Cell **16**, 609–618 (2004).
[25]N. Tanner (unpublished).
[26]L. Finzi and J. Gelles, "Measurement of lactose repressor-mediated loop formation and breakdown in single DNA molecules," Science **267**, 378–381 (1995).
[27]I. D. Vilfan, J. Lipfert, D. A. Koster, S. G. Lemay, and N. H. Dekker, "Magnetic tweezers for single-molecule experiments," in *Handbook of Single-Molecule Biophysics*, edited by P. Hinterdorfer and A. van Oijen (Springer, NY, 2009), pp. 371–395.
[28]J. G. Yodh, M. Schlierf, and T. Q. Ha, "Insight into helicase mechanism and function revealed through single-molecule approaches," Rev. Biophys. **43**, 185–217 (2010).
[29]W. H. Press, S. A. Teukolsky, W. T. Vetterling, and B. P. Flannery, *Numerical Recipes: The Art of Scientific Computing* (Cambridge U. P., New York, 2007), pp. 899–901.
[30]N. A. Tanner, S. M. Hamdan, S. Jergic, K. V. Loscha, P. M. Schaeffer, N. E. Dixon, and A. M. van Oijen, "Single-molecule studies of fork dynamics in Escherichia coli DNA replication," Nat. Struct. Mol. Biol. **15**, 170–176 (2008).
[31]Downloads are available at ⟨www.python.org⟩.
[32]Information on packages as well as downloads can be found at ⟨www.scipy.org⟩.

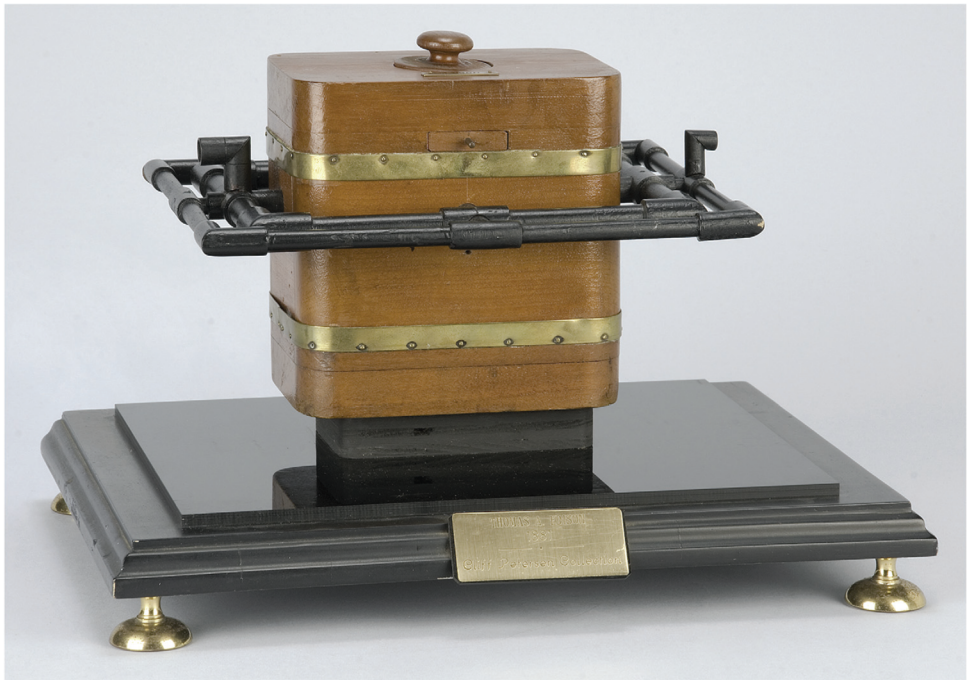

Carbonizer Model

From 1790 until 1880 inventors were required to submit a model of their inventions along with their application to the U. S. Patent Office. This model, submitted by Thomas A. Edison in 1881, consists of a rectangular box (representing an oven) in which a carbonizing flask is inserted. The latter is composed of two parts: the base with its numerous legs (like pegs on this model), which permits the heat from the carbonizer to circulate freely around the flask. On top of the base is arranged a series of plates containing the filaments to be carbonized.

The oven itself consists of a box, around which are pipes with inlets connected to it. The first layer of pipes is for a combustible gas, and the second is for pressurized air. A peep hole on top of the oven's cover is provided to observe the condition of the flask.

This model is a part of the Susan Mae Eichelberg(Glendening/ professional name, glendeningsusan@hotmail.com) collection, which includes over 400 patent models of historical significance. This patent model collection is one of the exhibits at The Riverbank Historic House Museum at 2 Riverbank Lane, Cornwall on Hudson, New York 12520. The images and this description are courtesy of the Collection of Historical Scientific Instruments, Department of the History of Science, President and Fellows of Harvard College, where these patent models were exhibited in 2009. See patentmodelmuseum.org.